

# Charm-Baryon Production in Proton-Proton Collisions

Min He<sup>a</sup>, Ralf Rapp<sup>b</sup>

<sup>a</sup>*Department of Applied Physics, Nanjing University of Science and Technology, Nanjing 210094, China*

<sup>b</sup>*Cyclotron Institute and Department of Physics & Astronomy, Texas A&M University, College Station, TX 77843, USA*

---

## Abstract

Recent measurements of charm-baryon production in proton-proton collisions at the LHC have found a surprisingly large yield relative to those of  $D$ -mesons. We propose that this observation can be explained by the statistical hadronization model (SHM), by employing a largely augmented set of charm-baryon states beyond the current listings of the particle data group. We estimate the additional states using guidance from the relativistic quark model and from lattice QCD. Using charm- and strange-quark fugacity factors to account for the well-known suppression of heavy flavor in elementary collisions, we compute the yields and spectra of  $D$ ,  $D_s$  and  $\Lambda_c$  hadrons in proton-proton collisions at  $\sqrt{s} = 5$  TeV. Our main finding is that the enhanced feeddown from excited charm baryons can account for the  $\Lambda_c/D^0$  ratio measured by ALICE at midrapidity, with some caveat for the forward-rapidity LHCb data. Furthermore, assuming independent fragmentation of charm quarks but with the hadronic ratios fixed by the SHM, the measured transverse-momentum ( $p_T$ ) spectra of  $D$ -mesons and  $\Lambda_c$  can also be described; in particular, the low- $p_T$  enhancement in the observed  $\Lambda_c/D^0$  ratio is attributed to the enhanced feeddown from “missing” charm-baryon states. We comment on the implications of these findings for measurements of  $D_s$  and  $\Lambda_c$  in heavy-ion collisions.

*Keywords:* Heavy Flavor Production, Proton-Proton Collisions, Charm Baryons

---

## 1. Introduction

The production of heavy-flavor (HF) particles in high-energy hadronic collisions is a versatile source of information on various aspects of Quantum Chromodynamics (QCD). The primordial pair production of heavy quarks and their anti-quarks in a hard partonic scattering event is a fruitful testing ground for perturbative QCD calculation. Based on collinear factorization, this process essentially governs the total heavy-quark (HQ) production cross section. On the other hand, the subsequent hadronization of charm ( $c$ ) and bottom ( $b$ ) quarks into HF hadrons is an inherently nonperturbative process related to, or even driven by, the confining property of QCD.

Various models to account for the different species of the observed HF hadrons have been put forward, including independent fragmentation models, usually applicable at sufficiently large momentum, or color neutralization models such as string fragmentation, color reconnection or color ropes [1, 2, 3, 4, 5, 6, 7, 8]. In addition, the statistical hadronization model (SHM) has been em-

ployed, essentially replacing the complexity of the hadronization process by thermo-statistical weights governed by the masses of available hadron states at a universal hadronization “temperature”,  $T_H$ . The SHM has been successfully applied to light- and strange-hadron production in both heavy-ion and elementary collisions, with the addition of a strangeness suppression factor,  $\gamma_s < 1$ , in the latter (and in peripheral heavy-ion collisions) [9, 10]. It also works for various charm-meson ratios [11, 12, 13, 14, 15, 16]. However, recent measurements of charm-baryon production in proton-proton ( $pp$ ) collisions by the ALICE collaboration at the LHC held a surprise; specifically, the cross section ratio of prompt  $\Lambda_c$  over  $D^0$ -mesons,  $\Lambda_c/D^0 \simeq 0.54$ , measured at  $\sqrt{s} = 7$  GeV [17] turns out to be much larger than expected in most event generators [2, 3, 4, 18, 19], as well as in the SHM where it is  $\sim 0.22$  [11] based on charm-hadron states listed by the particle data group (PDG) [20]. Recent attempts [7] to reproduce these data using an independent fragmentation approach confirmed the challenge to describe the ALICE data. Measure-

ments of  $\Lambda_c$  production have also been carried out by the LHCb collaboration at forward rapidities, yielding smaller values of  $\Lambda_c/D^0 \simeq 0.25 \pm 0.05$  in  $\sqrt{s} = 7$  TeV  $pp$  collisions [21], and  $\sim 0.35 \pm 0.05$  in  $\sqrt{s_{NN}} = 5$  TeV  $pPb$  collisions [22].

In the present paper we explore in how far the observed enhancement of  $\Lambda_c$  production can be due to hitherto unobserved charm-baryon states, not listed in the PDG tables [20]. For example, the latter currently contain 6  $\Lambda_c$  and 3  $\Sigma_c$  states, compared to 14  $\Lambda$  and 10  $\Sigma$  states (plus additional less certain states) in the strangeness sector. All of the observed excited single-charm baryons have dominant decay branchings into  $\Lambda_c$  final states with widths of the order of MeV, and thus their “feeddown” qualifies as “prompt”  $\Lambda_c$  production as measured in experiment. We will estimate the missing states by taking guidance from relativistic quark model (RQM) [23] calculations. We will implement the updated thermal yields to compute the hadro-chemistry of  $\Lambda_c$ ,  $D^0$ ,  $D^*$  and  $D_s$  yields, and also calculate their transverse-momentum ( $p_T$ ) spectra through fragmentation functions of a given  $c$ -quark spectrum adapted for mesons and baryons in the fixed-order-next-to-leading-log (FONLL) scheme [1, 5].

## 2. Charm-Baryon Spectrum and SHM

The issue of “missing resonances” is a long-standing problem in hadronic spectroscopy, in particular in the baryon sector [24]. For charm baryons, this problem is particularly challenging as direct spectroscopic measurements are rather scarce. Lattice-QCD (lQCD) computations [25] of the charm-baryon spectrum indeed show a vastly richer spectrum than currently measurable, with ten’s of additional states in the single-charm sector (most pertinent to our present work), approximately following quark model classifications of  $SU(6)$ - $O(3)$  flavor-spin-angular-momentum symmetry. More indirectly, the analysis of the partial pressure of open-charm states and charm-quark susceptibilities in thermal lQCD [26] also found that their results for temperatures  $T=150$ - $170$  MeV are much under-predicted using PDG states only, while the use of a charm-hadron spectrum predicted by the RQM [23] resulted in a good description.

Motivated by these findings we construct a SHM based on two different inputs for the charm-hadron states: (a) a PDG version of only including states listed in Ref. [20], and (b) a RQM version including additionally predicted charm-baryon states as listed

in Ref. [23], which amounts to an extra 18  $\Lambda_c$ ’s, 42  $\Sigma_c$ ’s, 62  $\Xi_c$ ’s, and 34  $\Omega_c$ ’s up to a mass of 3.5 GeV. We have checked that including additional RQM mesons would increase the thermal density of  $D^0$  by  $\sim 10\%$ , which does not affect our final results significantly. On the other hand, the baryon states in the RQM are based on a light-diquark scheme, which tends to give fewer states than a genuine three-quark picture [23] which could counter-balance an increase in excited  $D$ -meson states. As usual in the SHM, the thermal hadron densities follow from their masses,  $m_i$ , and spin-isospin degeneracies,  $d_i$ , evaluated at a hadronization temperature,  $T_H$ , as

$$n_i = \frac{d_i}{2\pi^2} m_i^2 T_H K_2\left(\frac{m_i}{T_H}\right), \quad (1)$$

where  $K_2$  is the modified Bessel function of second order. Given the agreement of the lQCD susceptibilities with the same RQM charm-baryon ensemble as used here up to temperatures of 170 MeV [26], we use the latter as an upper estimate of  $T_H$ , and utilize lower values as part of our error estimate. A flavor hierarchy in the operational hadronization temperature of the QCD crossover transition has been suggested before based on comparisons of light and strange-quark susceptibilities [27], amounting to an upward shift of about 15 MeV for strange hadrons.

An important ingredient are the branching ratios (BRs) of the excited charm hadrons to their ground states. For observed states, we use BRs as available from the PDG, and for “seen” decay channels without BRs we assume an equal weight. To explore the maximum effect of all RQM  $\Lambda_c$ ’s and  $\Sigma_c$ ’s not listed by the PDG, we assume that their decay chain always ends up with a ground-state  $\Lambda_c^+$  (plus one or two  $\pi$ ’s). This is motivated by the fact that the ground-state  $\Sigma_c(2455)$  is listed with a  $\sim 100\%$  BR into  $\Lambda_c + \pi$ , and by chiral-quark model studies [28] where the BR of  $D + N$  channels for several studied highly excited  $\Lambda_c$ ’s and  $\Sigma_c$ ’s were predicted to be very small compared to  $\Lambda_c + n\pi$  channels. For excited  $\Xi_c$ ’s (containing one strange quark) the PDG indicates  $\Lambda_c + K$  decay channels; lacking quantitative knowledge of those, we assume a 50% BR for the additional RQM  $\Xi_c$ ’s decaying to  $\Lambda_c$ , with the remaining 50% to the ground state  $\Xi_c$ . Finally, for the thermal densities of both  $D_s$  mesons and  $\Xi_c$  baryons, containing one strange (anti)quark, we apply a strangeness suppression factor of  $\gamma_s = 0.6$  in Eq. (1), in line with the empirical value of  $0.56 \pm 0.04$  extracted from  $\sqrt{s} = 200$  GeV  $pp$  collisions [29] (for  $\Omega_c$ ’s,  $\gamma_s^2$  is applied accordingly).

$n_i$ ( $\cdot 10^{-4}$ fm $^{-3}$ )	$D^0$	$D^+$	$D^{*+}$	$D_s^+$	$\Lambda_c^+$	$\Xi_c^{+,0}$	$\Omega_c^0$
PDG(170)	1.161	0.5098	0.5010	0.3165	0.3310	0.0874	0.0064
PDG(160)	0.4996	0.2223	0.2113	0.1311	0.1201	0.0304	0.0021
RQM(170)	1.161	0.5098	0.5010	0.3165	0.6613	0.1173	0.0144
RQM(160)	0.4996	0.2223	0.2113	0.1311	0.2203	0.0391	0.0044

Table 1: Thermal densities of “prompt” ground-state charmed hadrons for hadronization temperatures of  $T_H=170$  and 160 MeV (including strong feeddowns) in the PDG and RQM scenarios.

$f_i$	$D^0$	$D^+$	$D_s^+$	$\Lambda_c^+$
PDG(170)	0.4813	0.2113	0.1312	0.1372
PDG(160)	0.4968	0.2210	0.1304	0.1194
RQM(170)	0.4175	0.1834	0.1138	0.2379
RQM(160)	0.4473	0.1990	0.1174	0.1973

Table 2: Thermal fractions of  $D^0$ ,  $D^+$ ,  $D_s^+$  and  $\Lambda_c^+$  for hadronization temperatures of  $T_H=170$  and 160 MeV (including strong feeddowns) in the PDG and RQM scenarios.

$r_i$	$D^+/D^0$	$D^{*+}/D^0$	$D_s^+/D^0$	$\Lambda_c^+/D^0$
PDG(170)	0.4391	0.4315	0.2736	0.2851
PDG(160)	0.4450	0.4229	0.2624	0.2404
RQM(170)	0.4391	0.4315	0.2726	0.5696
RQM(160)	0.4450	0.4229	0.2624	0.4409

Table 3: Ratios of  $D^+$ ,  $D^{*+}$ ,  $D_s^+$  and  $\Lambda_c^+$  to  $D^0$  at  $T_H=170$  and 160 MeV (including strong feeddowns) in the PDG and RQM scenarios at two different hadronization temperatures.

The calculated thermal densities (with strong feeddowns) of the ground-state charm hadrons are summarized in Tab. 1, where we also include results for  $T_H = 160$  MeV. The densities are converted into fractions of the total charm content in Tab. 2. The additional baryon states in the RQM much enhance the fraction of the ground-state  $\Lambda_c$  in the system, relative to the PDG scenario, by about  $\sim 73\%$  (65%) at  $T_H = 170$  (160) MeV. We furthermore compute the ratios of  $D^+$ ,  $D^{*+}$ ,  $D_s^+$  and  $\Lambda_c^+$  to the  $D^0$ , as summarized in Tab. 3. The meson ratios are rather stable with respect to temperature variations, but the baryon-to-meson ratio is more sensitive. In the PDG scenario with  $T_H = 160$  MeV,  $\Lambda_c^+/D^0 \simeq 0.24$ , close to the previously reported SHM value of 0.22 obtained for  $T_H=156.5$  MeV [11, 30]. This value is increased to  $\Lambda_c^+/D^0 \simeq 0.57$  at  $T_H = 170$  MeV in the RQM scenario, almost doubling the PDG value and becoming comparable to the ALICE measurement [17]. This is one of the main results of our work.

In the following, we will keep the RQM scenario with  $T_H = 170$  MeV as our default and calculate the  $p_T$ -differential cross sections of charmed hadrons by fragmenting a universal underlying charm-quark  $p_t$  spectrum.

### 3. Fragmentation and Decay Simulation

As discussed in the introduction, the charm pair production, as a hard process, is believed to be governed by perturbative QCD, even down to low momenta. Therefore, our starting point to compute charm-hadron  $p_T$  spectra is the charm-quark  $p_t$  spectrum in  $pp$  collisions at  $\sqrt{s} = 5.5$  TeV as simulated by FONLL [1, 5] (we use it as a proxy for that at  $\sqrt{s} = 5.02$  TeV). We utilize it to perform fragmentation into various charmed mesons and baryons using the fragmentation function [31] that was also implemented in the FONLL framework,

$$D_{c \rightarrow H}(z) = N \frac{rz(1-z)^2}{[1-(1-r)z]^6} [(6-18(1-2r)z + (21-74r+68r^2)z^2 - 2(1-r)(6-19r+18r^2)z^3 + 3(1-r)^2(1-2r+2r^2)z^4)], \quad (2)$$

where  $z = p_T/p_t$  is the fraction of the hadron ( $H$ ) momentum ( $p_T$ ) relative to the quark momentum ( $p_t$ ), and the parameter  $r$  may be interpreted as the ratio of the mass of the fragmenting quark to the mass of the hadron [31]. The normalization,  $N$ , of the fragmentation function into each hadron is, however, determined according to the pertinent thermal densities calculated in the RQM scenario as

described in the previous section. The assumption here is that the phase-space population implied by the thermal model does not significantly affect the  $p_T$  spectrum of the hadrons emerging from the fragmentation of the primordial charm-quark spectrum (some of that effect is absorbed into our tuning of the  $r$  parameter described below).

We tune the parameter  $r$  in Eq. (2) for the ground-state  $D^0$  and  $\Lambda_c^+$  as to fit the experimental slope of their  $p_T$  spectra. Once  $r_{D^0}$  is fixed, the value of  $r$  for other  $D$  and  $D_s$  mesons ( $M$ ) follows from mass scaling:  $r_M/r_{D^0} = ((m_M - m_c)/m_M)/((m_{D^0} - m_c)/m_{D^0})$  [31], where  $m_c = 1.5$  GeV is the charm-quark mass used in our calculations. The same is done for charm baryons ( $B$ ) based on  $r_{\Lambda_c^+}: r_B/r_{\Lambda_c^+} = ((m_B - m_c)/m_B)/((m_{\Lambda_c^+} - m_c)/m_{\Lambda_c^+})$ . Through our fits the best  $r$ -values for the ground-state hadrons turn out to be  $r_{D^0}=0.1$  and  $r_{\Lambda_c^+}=0.16$ . Each charm hadron formed from fragmentation is then decayed into ground-state particles assuming a constant matrix element, with the decay kinematics solely determined by phase space, and the pertinent branching ratios discussed in Sec. 2.

To effectively conduct the fragmentation and decay simulations, we introduce an ‘‘average’’ baryon state to represent the additional RQM states of each category (*i.e.*, with the same isospin) by a combined spin degeneracy as the sum of the pertinent category, and an average mass that results in a thermal density corresponding to the sum of all states in that category. Specifically, 18 additional  $\Lambda_c$ ’s are represented by an ‘‘average’’  $\bar{\Lambda}_c^*$  of effective mass 3.17 GeV and total spin degeneracy of 43.5; 42 additional  $\Sigma_c$ ’s by an ‘‘average’’  $\bar{\Sigma}_c^*$  of effective mass 3.10 GeV and total spin degeneracy 88.5; 62 additional  $\Xi_c$ ’s by an ‘‘average’’  $\bar{\Xi}_c^*$  of effective mass 3.24 GeV and total spin degeneracy 135.5; and additional 34  $\Omega_c$ ’s by an ‘‘average’’  $\bar{\Omega}_c^*$  of effective mass 3.26 GeV and total spin degeneracy 65.5. To check the accuracy of this mass-averaging procedure, we have calculated the integrated yields of each ground-state particle from fragmentation plus decay simulations, and confirmed that the pertinent fractions and ratios agree with those calculated from the explicit RQM particle content (as listed in Tabs. 2 and 3) within a few percent.

### 3.1. LHC

The results of the fits of the fragmentation and decay simulations in both PDG and RQM scenarios

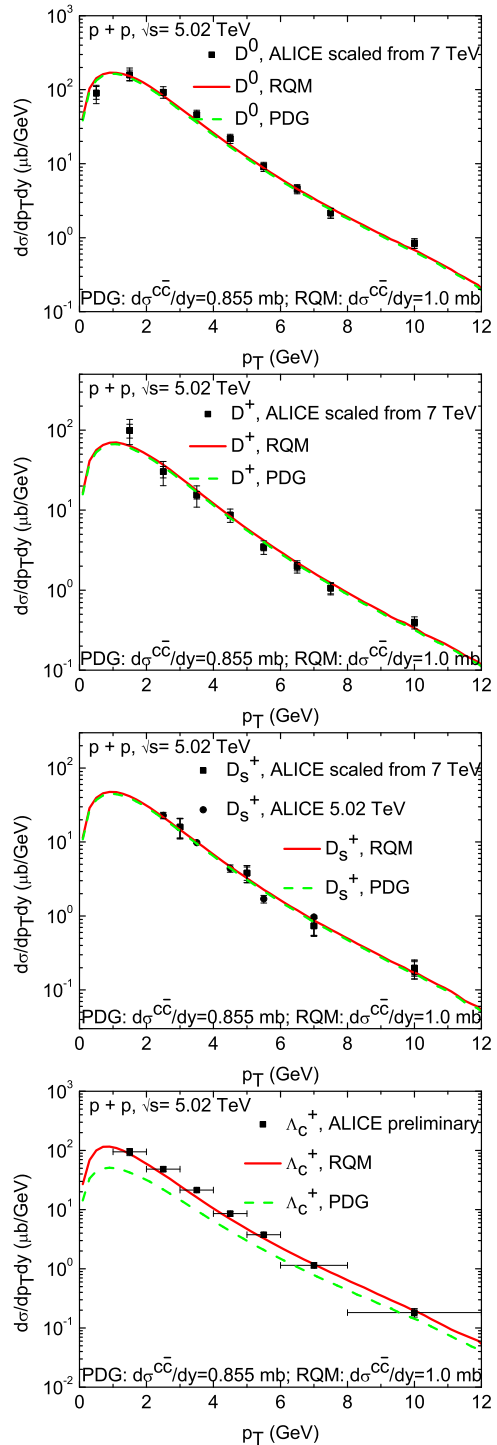


Figure 1: (Color online) Cross sections of  $D^0$ ,  $D^+$ ,  $D_s^+$  and  $\Lambda_c^+$  (including strong feeddowns) as a function of transverse momentum in  $\sqrt{s} = 5.02$  TeV  $pp$  collisions. The PDG (dashed green lines) and RQM scenario (solid red lines) with  $T_H = 170$  MeV are compared to ALICE data at mid-rapidity [14, 16, 17].

with  $T_H = 170$  MeV to the  $p_T$ -differential cross sections,  $d\sigma/dp_T dy$ , for  $D^0$ ,  $D^+$ ,  $D_s^+$  and  $\Lambda_c^+$ , as measured by ALICE in  $\sqrt{s} = 5.02$  TeV  $pp$  collisions, are shown in Fig. 1 together with the data [14, 16, 17]. The fitted total charm cross sections turn out to be  $d\sigma^{c\bar{c}}/dy = 0.855$  mb and 1.0 mb in these two scenarios, respectively. While the meson spectra can be well reproduced within the PDG scenario, the  $\Lambda_c^+$  spectrum exhibits a substantial deficiency in this scenario. Including the additional RQM baryons makes a decisive difference and enables a good description of the  $\Lambda_c^+$  spectrum measured by ALICE. Also note that the decay feeddown leads to an appreciable low- $p_T$  enhancement over the PDG scenario that seems to be supported by the ALICE data.

Next, we turn to the  $\Lambda_c^+/D^0$  ratio following from our fit, shown in Fig. 2. The ALICE data [17] at mid-rapidity confirm that the RQM scenario is clearly favored, including the increasing trend toward lower  $p_T$  as referred to above. On the other hand, the LHCb data [21] at forward rapidity are better reproduced by the PDG scenario. Possible reasons for this may be the reduced particle multiplicity, *i.e.*, the fewer production of light quarks and antiquarks at forward rapidity, which limits the phase space available for charm-quark coalescence especially for more massive resonances, or a lower hadronization temperature [32]. Interestingly, the LHCb data in  $p$ -Pb collisions [22] show an increase in this ratio, and possibly also a rising trend toward central rapidity, while the ALICE  $p$ -Pb data at midrapidity are consistent with their  $pp$  data [17], possibly exhibiting a slight hardening.

### 3.2. Predictions at RHIC energy

We repeat our fragmentation and decay simulation in the RHIC energy regime, for  $\sqrt{s} = 200$  GeV  $pp$  collisions, with the same parameters for both PDG and RQM scenarios at  $T_H = 170$  MeV. The only change is the underlying charm-quark  $p_t$  spectrum which we again adopt from the FONLL framework, and the total charm input cross section. The thus obtained  $p_T$  spectrum for  $D^0$ 's is plotted in Fig. 3 and shows good agreement with STAR data [33, 34]. The fitted charmed cross section turns out to be  $d\sigma^{c\bar{c}}/dy = 0.221$  (0.189) mb in the RQM (PDG) scenario. The pertinent predictions for the  $\Lambda_c^+/D^0$  ratio are displayed in Fig. 3, showing very similar features as at LHC energies.

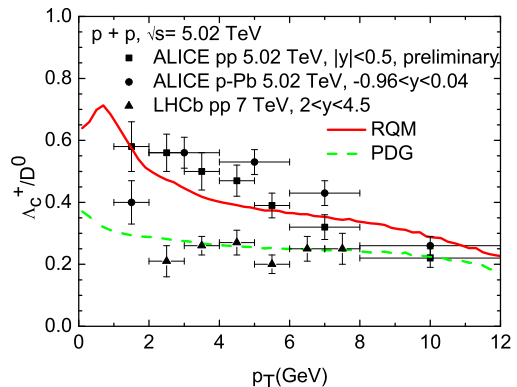


Figure 2: (Color online) The  $\Lambda_c^+/D^0$  ratio following from our fits in the PDG (dashed green line) and RQM (solid red line) scenario at  $T_H = 170$  MeV in  $\sqrt{s} = 5.02$  TeV  $pp$  collisions, compared to ALICE [17] and LHCb [21] data.

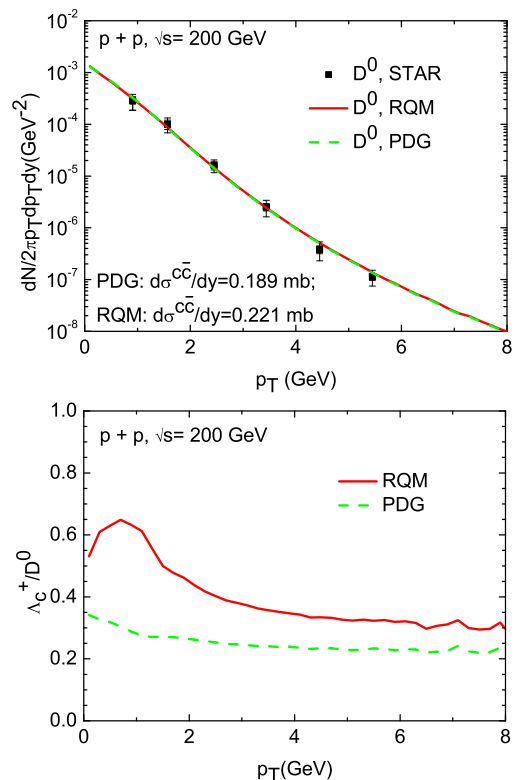


Figure 3: (Color online) The  $p_T$  spectrum of  $D^0$ 's (upper panel) and the  $\Lambda_c^+/D^0$  ratio (lower panel) in  $\sqrt{s} = 200$  GeV  $pp$  collisions from PDG and RQM scenarios at  $T_H = 170$  MeV, together with STAR  $D^0$  data in the upper panel [33, 34].

## 4. Summary

We have employed the statistical hadronization model to compute the hadro-chemistry of charm hadrons in  $pp$  collisions at collider energies. In particular, we have augmented the underlying charm-baryon spectrum by a relatively large number of states as predicted by the relativistic quark model. A related issue is well known for the spectroscopy of light and strange baryons, where many more states are observed than in the charm sector. The need for additional charm-baryon states is further supported by lattice-QCD computations of the vacuum spectrum and of thermal charm susceptibilities in the vicinity of the transition temperature. Utilizing the RQM spectrum, we have found a marked increase of the  $\Lambda_c/D^0$  ratio over the predictions based on known states. As a result, the surprising enhancement of  $\Lambda_c$  production as found by the ALICE collaboration in  $\sqrt{s} = 7$  TeV  $pp$  collisions at midrapidity can be explained within the theoretical and experimental uncertainties (the smaller enhancement found at forward rapidities by the LHCb collaboration may hint at limitations of this picture). We have also computed pertinent  $p_T$  spectra using the fragmentation function formalism but with the hadron ratios determined by the SHM. Also here a good agreement with data has been found, including a low- $p_T$  enhancement for the  $\Lambda_c$  which we attribute to feeddown from excited states.

Our findings suggest several directions of future work. The augmented SHM can be tested by other charm hadrons (such as  $\Sigma_c$  or  $\Xi_c$ ) in  $pp$  and  $p$ -A collision. It also has predictive power for the bottom sector. Furthermore, we expect that our findings have important ramifications for the understanding of the charm (and bottom) hadro-chemistry and kinetics in heavy-ion collisions. The intense rescattering of charm (and presumably also bottom) quarks in the hot QCD medium, as reflected by the nuclear modification factor and large elliptic flow of  $D$ -mesons in Au-Au and Pb-Pb collisions at RHIC and the LHC, stipulates the need for a controlled and universal equilibrium limit in transport calculations of the spectra and yields of charm hadrons at low and intermediate  $p_T$  [35]. We believe that our analysis presented here provides a significant and well-motivated improvement in this direction, not only for understanding  $\Lambda_c$  production [36, 37], but also for current and future measurements of a much richer set of charm ( $D_s$ ,  $\Sigma_c$ , ...) and bottom ( $B_s$ ,  $\Lambda_b$ ,  $\Sigma_b$ ,

...) hadrons.

**Acknowledgments:** This work was supported by the NSFC under grant 11675079 (MH), and by the U.S. National Science Foundation (NSF) under grant no. PHY-1614484 (RR).

## References

- [1] M. Cacciari, M. Greco and P. Nason, JHEP **9805**, 007 (1998).
- [2] B. A. Kniehl, G. Kramer, I. Schienbein and H. Spiesberger, Eur. Phys. J. C **41**, 199 (2005).
- [3] S. Frixione, P. Nason and G. Ridolfi, JHEP **0709**, 126 (2007).
- [4] B. A. Kniehl, G. Kramer, I. Schienbein and H. Spiesberger, Eur. Phys. J. C **72**, 2082 (2012).
- [5] M. Cacciari, S. Frixione, N. Houdeau, M. L. Mangano, P. Nason and G. Ridolfi, JHEP **1210**, 137 (2012).
- [6] G. Kramer and H. Spiesberger, Nucl. Phys. B **925**, 415 (2017).
- [7] R. Maciula and A. Szczurek, Phys. Rev. D **98**, no. 1, 014016 (2018).
- [8] I. Helenius and H. Paukkunen, JHEP **1805**, 196 (2018).
- [9] P. Braun-Munzinger, K. Redlich and J. Stachel, "Particle production in heavy ion collisions," In \*Hwa, R.C. (ed.) et al.: Quark gluon plasma\* 491-599, [nucl-th/0304013].
- [10] A. Andronic, P. Braun-Munzinger, K. Redlich and J. Stachel, Nature **561**, no. 7723, 321 (2018).
- [11] A. Andronic, P. Braun-Munzinger, K. Redlich and J. Stachel, Phys. Lett. B **659**, 149 (2008).
- [12] A. Andronic, F. Beutler, P. Braun-Munzinger, K. Redlich and J. Stachel, Phys. Lett. B **678**, 350 (2009).
- [13] S. Acharya *et al.* [ALICE Collaboration], JHEP **1810**, 174 (2018).
- [14] J. Adam *et al.* [ALICE Collaboration], Phys. Rev. C **94**, 054908 (2016).
- [15] S. Acharya *et al.* [ALICE Collaboration], Eur. Phys. J. C **77**, no. 8, 550 (2017).
- [16] S. Acharya *et al.* [ALICE Collaboration], arXiv:1901.07979 [nucl-ex].
- [17] S. Acharya *et al.* [ALICE Collaboration], JHEP **1804**, 108 (2018); Elisa Meninno on behalf of the ALICE Collaboration, PoS (HardProbes2018) 137, <https://pos.sissa.it/345/137/>.
- [18] J. R. Christiansen and P. Z. Skands, JHEP **1508**, 003 (2015).
- [19] C. Bierlich and J. R. Christiansen, Phys. Rev. D **92**, no. 9, 094010 (2015).
- [20] M. Tanabashi *et al.* [Particle Data Group], Phys. Rev. D **98**, no.3, 030001 (2018).
- [21] R. Aaij *et al.* [LHCb Collaboration], Nucl. Phys. B **871**, 1 (2013).
- [22] R. Aaij *et al.* [LHCb Collaboration], arXiv:1809.01404 [hep-ex].
- [23] D. Ebert, R. N. Faustov and V. O. Galkin, Phys. Rev. D **84**, 014025 (2011).
- [24] V. Crede and W. Roberts, Rept. Prog. Phys. **76**, 076301 (2013).
- [25] P. Madanagopalan, R. G. Edwards, N. Mathur and M. J. Peardon, PoS LATTICE **2014**, 084 (2015).

- [26] A. Bazavov *et al.*, Phys. Lett. B **737**, 210 (2014).
- [27] R. Bellwied, S. Borsanyi, Z. Fodor, S. D. Katz and C. Ratti, Phys. Rev. Lett. **111**, 202302 (2013).
- [28] X. H. Zhong and Q. Zhao, Phys. Rev. D **77**, 074008 (2008).
- [29] B. I. Abelev *et al.* [STAR Collaboration], Phys. Rev. C **79**, 034909 (2009).
- [30] A. Andronic, priv. comm. (2018).
- [31] E. Braaten, K. m. Cheung, S. Fleming and T. C. Yuan, Phys. Rev. D **51**, 4819 (1995).
- [32] F. Becattini and J. Cleymans, J. Phys. G **34** S959 (2007).
- [33] L. Adamczyk *et al.* [STAR Collaboration], Phys. Rev. D **86**, 072013 (2012).
- [34] L. Adamczyk *et al.* [STAR Collaboration], Phys. Rev. Lett. **113**, no. 14, 142301 (2014); Erratum: [Phys. Rev. Lett. **121**, no. 22, 229901 (2018)]
- [35] R. Rapp, arXiv:1901.06440 [nucl-th].
- [36] S. Acharya *et al.* [ALICE Collaboration], arXiv:1809.10922 [nucl-ex].
- [37] L. Zhou [STAR Collaboration], Nucl. Phys. A **967**, 620 (2017).